JACS
JOURNAL OF THE AMERICAN CHEMICAL SOCIETY

COMMUNICATION

pubs.acs.org/JACS

Enhanced Thermal Stability and Magnetic Properties in NaCl-Type FePt−MnO Binary Nanocrystal Superlattices

Angang Dong,*[,†,⊥] Jun Chen,[‡,⊥] Xingchen Ye,[§] James M. Kikkawa,[∥] and Christopher B. Murray*[,‡,§]

[†]The Molecular Foundry, Lawrence Berkeley National Laboratory, Berkeley, California 94720, United States

[‡]Department of Materials Science and Engineering, [§]Department of Chemistry, and [∥]Department of Physics and Astronomy, University of Pennsylvania, Philadelphia, Pennsylvania 19104, United States

Supporting Information

ABSTRACT: We report the growth of NaCl-type binary nanocrystal (NC) superlattice membranes by coassembly of FePt and MnO NCs at the liquid−air interface. The constituent FePt NCs were converted into the hard magnetic $L1_0$ phase by thermal annealing at 650 °C without degradation of the long-range NC ordering. In contrast, both FePt-only NC superlattices and FePt−MnO disordered NC mixtures showed substantial FePt sintering under the same annealing conditions. Our results demonstrate that the incorporation of FePt NCs into binary superlattices can solve the problems of FePt sintering during conversion to the $L1_0$ phase, opening a new route to the fabrication of ordered ferromagnetic NC arrays on a desired substrate for high-density data storage applications.

Two-dimensional (2D) ordered arrays or superlattices consisting of hard magnetic nanocrystals (NCs) are well-suited for high-density magnetic data storage applications.[1−5] $L1_0$-phase face-centered-tetragonal (fct) FePt exhibits large uniaxial magnetocrystalline anisotropy ($\sim 7 \times 10^6$ J m^{-3}) and high coercivity, making it a key candidate for future ultrahigh-density magnetic recording media.[6] Chemically synthesized FePt NCs possess excellent size monodispersity and tunability and can also form superlattices by self-assembly.[7−10] However, the as-synthesized FePt NCs typically have a face-centered cubic (fcc) crystal structure,[7] rendering them unsuitable for use in data storage because of the superparamagnetic property of fcc-FePt at room temperature. The fcc-to-fct phase transformation requires high-temperature (>550 °C) annealing,[7] which unfortunately leads to severe FePt agglomeration and sintering, thus degrading the NC size uniformity and ordering.[10−12] Therefore, realizing the fcc-to-fct transition without sintering of the FePt NCs is one of the major challenges in the production of FePt-based magnetic recording materials.[3]

Much effort has been devoted to seeking the solution to sintering problems,[13−21] aiming to assemble $L1_0$-phase FePt NC arrays with well-defined particle positioning and interparticle separation. One strategy is to coat FePt NCs with a thermally stable material such as SiO_2,[13,14] MnO,[15] or MgO,[16,17] which serves as a physical barrier that prevents FePt sintering during heat treatment. Despite the largely reduced NC agglomeration, surface modification of FePt NCs makes their further assembly into long-range-ordered arrays difficult.[13−17] Alternatively, fct-FePt NCs can be obtained by growth of fcc-FePt NCs confined in a hard template (e.g., mesoporous silica) followed by thermal annealing.[19−21] Although small domains of relatively ordered fct-FePt NC arrays can be achieved, this approach cannot be applied to the fabrication of large-area 2D FePt arrays on a desired substrate because of the use of irregularly shaped templates.[19−21] In this work, we report that 2D long-range-ordered $L1_0$-phase FePt NC arrays can be realized by coassembly of FePt and MnO NCs into NaCl-type binary NC superlattice (BNSL) membranes. The resulting BNSLs exhibit significantly enhanced thermal stability relative to either FePt-only NC superlattices or disordered FePt−MnO NC mixtures. Thermal annealing of FePt−MnO BNSL membranes at 650 °C causes the fcc-to-fct phase transition of FePt NCs while preserving the ordered structure of the BNSLs, resulting in ferromagnetic membranes with in-plane coercivities as high as 5 kOe at room temperature.

MnO NCs were chosen to coassemble with FePt NCs into BNSLs because MnO is a thermally stable antiferromagnetic material with a rather high melting point (~2000 °C) that has previously been demonstrated to prevent the sintering of FePt NCs through the formation of core−shell structures.[15] Although the BNSL structure can be adjusted by tuning the size and number ratios of the two NC components,[22] we note that the NaCl-type binary superlattice consisting of large MnO NCs and small FePt NCs is an ideal structure to prevent FePt sintering. In this cubic structure, each FePt NC is located in the center of an octahedron consisting of six MnO NCs (Figure 1a)[23] that provides a thermally stable barrier to block the migration and aggregation of FePt NCs during conversion to the $L1_0$ phase.

NaCl-type FePt−MnO BNSL membranes were grown using the recently developed liquid−air interfacial assembly approach.[24] Briefly, a colloidal dispersion containing 3.5 nm FePt NCs[7] and 13 nm MnO NCs[25] (Figure S1 in the Supporting Information) in hexane was spread on the surface of diethylene glycol (DEG). The growth of BNSL membranes was induced by hexane evaporation, and the membrane thickness could be tuned by varying the NC concentration (Figure S2).[26] The BNSL membranes obtained could readily be transferred from the DEG surface to a desired substrate, enabling structural characterization, thermal annealing, and magnetic property measurements.[27] Figure 1b shows typical transmission electron microscopy (TEM) images of a (111)-oriented NaCl-type BNSL membrane consisting of one layer of FePt NCs sandwiched between two MnO NC layers. A side view

Received: June 20, 2011
Published: August 01, 2011

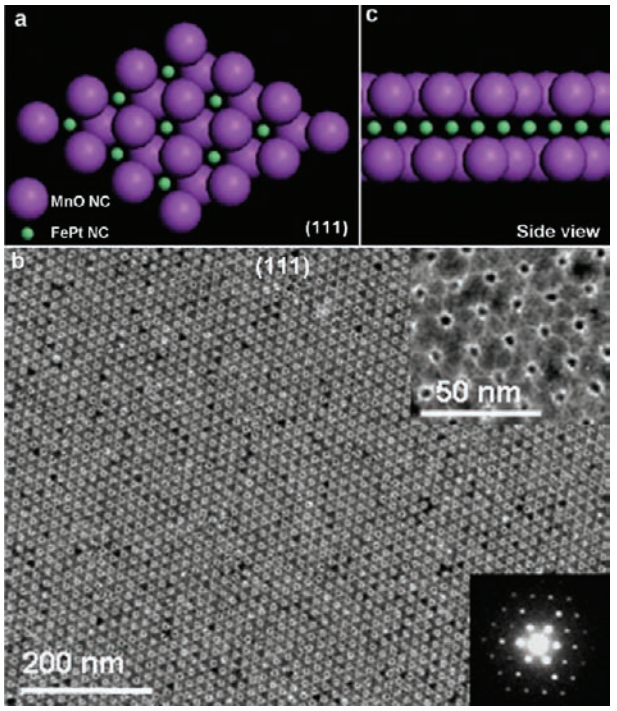

Figure 1. (a) Structural model of the (111)-oriented NaCl-type BNSL viewed from the top. (b) TEM image of the as-made NaCl-type FePt−MnO BNSL membrane with the (111) lattice projection oriented parallel to the TEM grid. The top-right inset shows a magnified TEM view, and the bottom-right inset is the SAED pattern. (c) Schematic illustration of a side view of the TEM image.

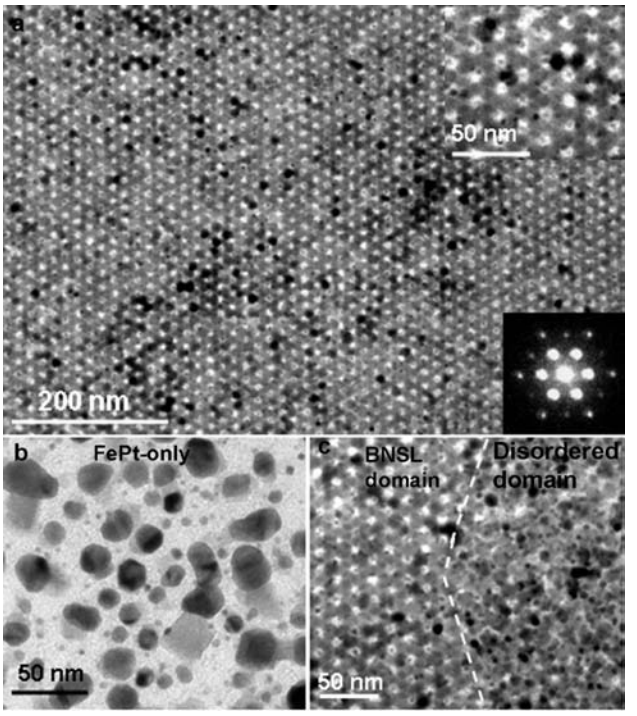

Figure 2. TEM images of the thermally annealed samples. (a) FePt−MnO BNSL membrane. The top-right and bottom-right insets are a magnified TEM view and the SAED pattern, respectively. (b) FePt-only NC superlattices. (c) FePt−MnO NC membrane containing both a BNSL domain and a disordered NC mixture domain. The dashed line indicates the boundary between the two domains.

of the membrane is illustrated schematically in Figure 1c. Because of the contrast difference, each individual FePt NC located in the center of an octahedron consisting of six MnO NCs can be clearly observed (Figure 1b, top-right inset). TEM, small-angle electron diffraction (SAED) (Figure 1b, bottom-right inset), and high-resolution scanning electron microscopy (HRSEM) (Figure S3a) confirmed that the NaCl-type BNSL membranes were predominantly oriented in the (111) lattice projection with the membrane surface terminated by MnO NCs.

To convert FePt NCs into the $L1_0$ phase, the BNSL membranes were transferred to SiO_2-coated TEM grids or SiO_2−Si wafers and then subjected to rapid thermal annealing under vacuum at 650 °C for 30 min. TEM demonstrated that the long-range ordering of the BNSLs was well-preserved without an obvious morphology change in either NC component after annealing (Figure 2a and Figure S4), as further confirmed by SAED (Figure 2a, bottom-right inset) and HRSEM (Figure S3b). The presence of isolated FePt NCs indicates that they survived the high-temperature annealing process without sintering. In contrast, the FePt-only NC superlattices (Figure S1a) were severely sintered under the same annealing conditions (Figure 2b), consistent with previous results.[12] To evaluate further the thermal stability of the BNSLs, a FePt−MnO NC membrane consisting of both BNSL domains and disordered NC mixture domains was prepared in a control experiment by slightly increasing the hexane evaporation rate. Notably, the disordered domains showed clear signs of FePt agglomeration after thermal annealing (Figure 2c and Figure S5), although the sintering appeared to be less severe than in the FePt-only sample, whereas the BNSL domains in the same membrane retained both NC size

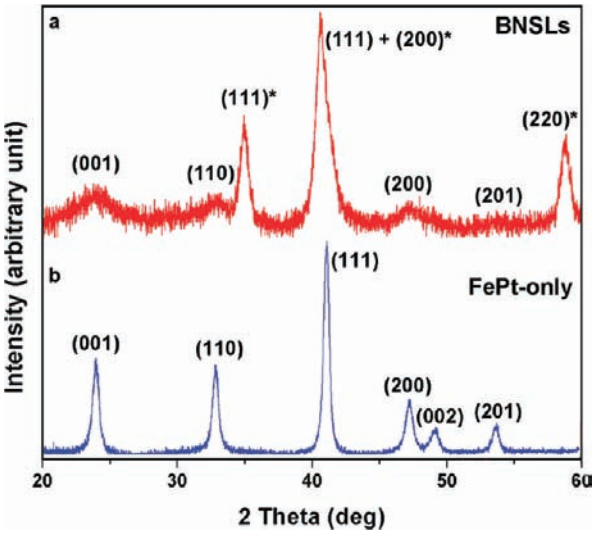

Figure 3. XRD patterns of thermally annealed samples. (a) FePt−MnO BNSL membrane. The diffraction peaks of MnO NCs are indicated by asterisks. (b) FePt-only NC superlattice.

uniformity and structure ordering. This provides strong evidence of the substantially enhanced thermal stability in BNSLs. We attribute this to the high degree of ordering in NaCl-type BNSLs, in which the spatially confined FePt NCs have much less probability to coalesce in comparison with the disordered NC mixtures. It should be mentioned that further increasing the

dx.doi.org/10.1021/ja2057314 |J. Am. Chem. Soc. 2011, 133, 13296–13299

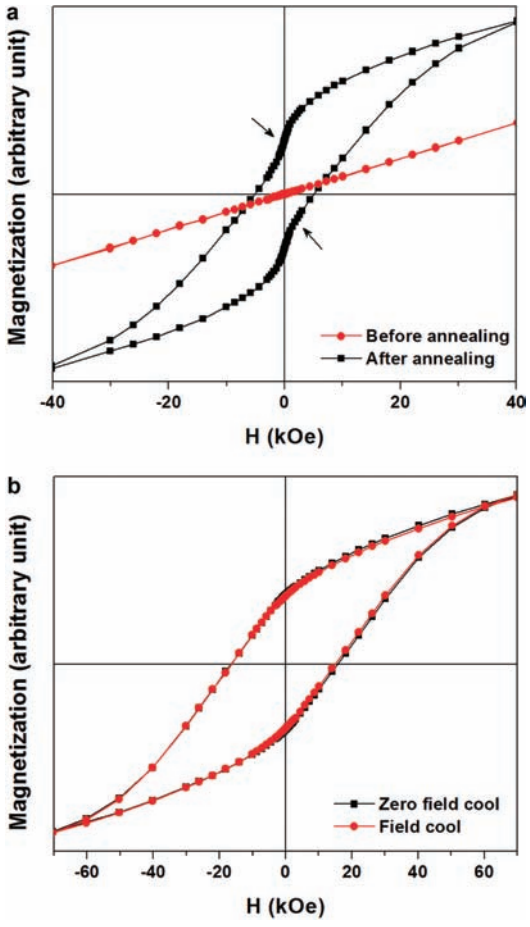

Figure 4. (a) Room-temperature hysteresis loops of FePt−MnO BNSL membranes before (red circle) and after (black square) annealing. The arrows indicate slight kinks arising from the soft magnetic components. (b) Low-temperature (5 K) hysteresis loops of annealed FePt−MnO BNSL membranes collected without (black square) and with (red circle) the presence of a magnetic field.

annealing temperature above 650 °C should gradually degrade the ordering of BNSLs with noticeable FePt sintering.

Figure 3a shows the powder X-ray diffraction (PXRD) pattern of a thermally annealed FePt−MnO BNSL transferred to a SiO_2−Si wafer. The diffraction peaks assigned to the $L1_0$-phase FePt NCs and rock-salt MnO NCs can be clearly identified, indicating the successful fcc-to-fct transition of the FePt NCs. In comparison with the PXRD pattern for the annealed FePt-only sample (Figure 3b), the much broader peaks for the BNSL are consistent with the nonsintering behavior of the FePt NCs observed using TEM.

Magnetic measurements on BNSL membranes transferred to SiO_2−Si wafers were carried out using a superconducting quantum interference device (Quantum Design) with the applied magnetic field parallel to the substrate. The magnetization curve indicates that the as-made FePt−MnO BNSL membranes exhibited superparamagnetic behavior at room temperature (Figure 4a, red circle), as expected since the constituent FePt and MnO NCs are both superparamagnetic.[7,28] After vacuum thermal annealing at 650 °C for 30 min, the BNSL membranes became ferromagnetic, with an in-plane coercivity of 5 kOe at room temperature (Figure 4a, black square). Since MnO NCs do not show hysteresis behavior after thermal annealing (Figure S6), the high coercivity exhibited by BNSL membranes is solely due to the $L1_0$-phase FePt NCs. We note that there are slight kinks in the magnetic hysteresis loop for the BNSL membranes (arrows in Figure 4a), suggesting a soft magnetic component that coexists with the $L1_0$-phase FePt, which probably results from the composition inhomogeneity of the FePt NCs.[15] Nevertheless, a room-temperature coercivity value of 5 kOe is remarkable considering the small diameter (3.5 nm) of the nonsintered FePt NCs.[7,15] The coercivity of the BNSL membranes increased dramatically with decreasing temperature, reaching 16 kOe at 5 K (Figure S7).

It is also worth mentioning that we did not observe an exchange-bias effect in the FePt−MnO BNSLs. The low-temperature (5 K) hysteresis loop of a thermally annealed BNSL membrane collected by cooling the sample under an external magnetic field of 50 kOe is shown in Figure 4b (red circle). The hysteresis loop is essentially the same as the one collected in the absence of the magnetic field (Figure 4b, black square), without an apparent shift in the magnetization curve. This is distinct from the behavior of the previously reported FePt−MnO core−shell NC system, where exchange-bias behavior, as manifested by a shift in the magnetization curve of FePt NCs, was observed.[15] In that study, the exchange-bias effect was attributed to the magnetic exchange anisotropy between the ferromagnetic and antiferromagnetic NC components occurring at the core−shell atomic interface.[15,29] The absence of exchange bias in these thermally annealed FePt−MnO BNSL membranes suggests that the two NC components were not in direct contact, as also revealed in the TEM images, where the gap between FePt and MnO NCs can be readily observed (Figure 2a and Figure S4). This provides additional evidence that the BNSL structure is well-preserved without NC sintering upon thermal annealing. We suspect that the hard axes of the $L1_0$-phase FePt NCs were random, which would account for the nonsquare shape of the hysteresis curve.

In summary, coassembly of FePt and MnO NCs at the liquid−air interface yields long-range-ordered NaCl-type BNSL membranes that exhibit remarkable thermal stability relative to either FePt-only NC superlattices or disordered FePt−MnO NC mixtures. Thermal annealing at 650 °C converts the constituent FePt NCs into the magnetic hard $L1_0$ phase while preserving the NC ordering. The assembly approach can be readily extended to other $L1_0$-phase NCs such as $CoPt_3$ and FePd,[30,31] opening a new and general route to the fabrication of highly ordered 2D ferromagnetic NC arrays on a desired substrate for high-density data storage applications.

■ ASSOCIATED CONTENT

Supporting Information. Methods (synthesis of colloidal NCs, self-assembly of FePt−MnO BNSL membranes, and instrumentation), additional TEM and HRSEM images, XRD patterns, and hysteresis loops. This material is available free of charge via the Internet at http://pubs.acs.org.

■ AUTHOR INFORMATION

Corresponding Author
adong@lbl.gov; cbmurray@sas.upenn.edu

Author Contributions
⊥These authors contributed equally.

■ ACKNOWLEDGMENT

The authors acknowledge the support from the U.S. Army Research Office (ARO) under Award MURI W911NF-08-1-0364. The work performed at the Molecular Foundry was supported by the U.S. Department of Energy, Office of Science, Office of Basic Energy Sciences, Scientific User Facilities Division, under Contract DE-AC02-05CH11231. J.C. acknowledges the DOE Office of ARPA-E for partial support under Award DE-AR0000123. X.Y. acknowledges support from the Department of Energy Basic Energy Sciences Division through Award DE-SC0002158. J.M.K. acknowledges the support from the NSF MRSEC Program under Award DMR-0520020. C.B.M. is grateful to the Richard Perry University Professorship for the support of his supervisor role.

■ REFERENCES

(1) Ross, C. *Annu. Rev. Mater. Res.* **2001**, *31*, 203.
(2) Terris, B. D.; Thomson, T. *J. Phys. D: Appl. Phys.* **2005**, *38*, R199.
(3) Wang, J. P. *Proc. IEEE* **2008**, *96*, 1847.
(4) Sun, S. *Adv. Mater.* **2006**, *18*, 393.
(5) Zeng, H.; Li, J.; Liu, J. P.; Wang, Z. L.; Sun, S. *Nature* **2002**, *420*, 395.
(6) Inomata, K.; Sawa, T.; Hashimoto, S. *J. Appl. Phys.* **1988**, *64*, 2537.
(7) Sun, S.; Murray, C. B.; Weller, D.; Folks, L.; Moser, A. *Science* **2000**, *287*, 1989.
(8) Shevchenko, E.; Talapin, D.; Kornowski, A.; Wiekhorst, F.; Kotzler, J.; Haase, M.; Rogach, A.; Weller, H. *Adv. Mater.* **2002**, *14*, 287.
(9) Kang, S.; Harrell, J. W.; Nikles, D. E. *Nano Lett.* **2002**, *2*, 1033.
(10) Varanda, L. C.; Jafelicci, M. *J. Am. Chem. Soc.* **2006**, *128*, 11062.
(11) Wang, H.; Zhou, M.; Yang, F.; Wang, J.; Jiang, Y.; Wang, Y.; Wang, H.; Li, Q. *Chem. Mater.* **2009**, *21*, 404.
(12) Dai, Z. R.; Sun, S.; Wang, Z. L. *Nano Lett.* **2001**, *1*, 443.
(13) Lee, D. C.; Mikulec, F. V.; Pelaez, J. M.; Koo, B.; Korgel, B. A. *J. Phys. Chem. B* **2006**, *110*, 11160.
(14) Yu, C. H.; Caiulo, N.; Lo, C. C. H.; Tam, K.; Tsang, S. C. *Adv. Mater.* **2006**, *18*, 2312.
(15) Kang, S.; Miao, G. X.; Shi, S.; Jia, Z.; Nikles, D. E.; Harrell, J. W. *J. Am. Chem. Soc.* **2006**, *128*, 1042.
(16) Kim, J.; Rong, C.; Lee, Y.; Liu, J. P.; Sun, S. *Chem. Mater.* **2008**, *20*, 7242.
(17) Kim, J.; Rong, C.; Liu, J. P.; Sun, S. *Adv. Mater.* **2009**, *21*, 906.
(18) Liu, C.; Wu, X.; Klemmer, T.; Shukla, N.; Weller, D.; Roy, A. G.; Tanase, M.; Laughlin, D. *Chem. Mater.* **2005**, *17*, 620.
(19) Kockrick, E.; Krawiec, P.; Schnelle, W.; Geiger, D.; Schappacher, F. M.; Pottgen, R.; Kaskel, S. *Adv. Mater.* **2007**, *19*, 3021.
(20) Gupta, G.; Patel, M. N.; Ferrer, D.; Heitsch, A. T.; Korgel, B. A.; Jose-Yacaman, M.; Johnston, K. P. *Chem. Mater.* **2008**, *20*, 5005.
(21) Kang, E.; Jung, H.; Park, J.; Kwon, S.; Shim, J.; Sai, H.; Wiesner, U.; Kim, J. K.; Lee, J. *ACS Nano* **2011**, *5*, 1018.
(22) Shevchenko, E. V.; Talapin, D. V.; Kotov, N. A.; O'Brien, S.; Murray, C. B. *Nature* **2006**, *439*, 55.
(23) Saunders, A. E.; Korgel, B. A. *ChemPhysChem* **2005**, *6*, 61.
(24) Dong, A.; Chen, J.; Vora, P. M.; Kikkawa, J. M.; Murray, C. B. *Nature* **2010**, *466*, 474.
(25) Park, J.; An, K. J.; Hwang, Y. S.; Park, J. G.; Noh, H. J.; Kim, J. Y.; Park, J. H.; Hwang, N. M.; Hyeon, T. *Nat. Mater.* **2004**, *3*, 891.
(26) Dong, A.; Ye, X.; Chen, J.; Murray, C. B. *Nano Lett.* **2011**, *11*, 1804.
(27) Chen, J.; Dong, A.; Cai, J.; Ye, X.; Kang, Y.; Kikkawa, J. M.; Murray, C. B. *Nano Lett.* **2010**, *10*, 5103.
(28) Schladt, T. D.; Schneider, K.; Shukoor, M. I.; Natalio, F.; Bauer, H.; Tahir, M. N.; Weber, S.; Schreiber, L. M.; Schroder, H. C.; Muller, W. E. G.; Tremel, W. *J. Mater. Chem.* **2010**, *20*, 8297.
(29) Bodnarchuk, M. I.; Kovalenko, M. V.; Groiss, H.; Resel, R.; Reissner, M.; Hesser, G.; Lechner, R. T.; Steiner, W.; Schaffler, F.; Heiss, W. *Small* **2009**, *5*, 2247.
(30) Shevchenko, E. V.; Talapin, D. V.; Rogach, A. L.; Kornowski, A.; Haase, M.; Weller, H. *J. Am. Chem. Soc.* **2002**, *124*, 11480.
(31) Hou, Y.; Kondoh, H.; Kogure, T.; Ohta, T. *Chem. Mater.* **2004**, *16*, 5149.